Original Article

Expression of *EGFR*-mutant proteins and genomic evolution in *EGFR*-mutant transformed small cell lung cancer

Shi-Ling Zhang[1,3#], Chan-Yuan Zhang[1,3#], Yu-Qing Chen[2,3#], Yu-Fa Li[4], Zhi Xie[3], Xu-Chao Zhang[3], Qing Zhou[3], Wen-Zhao Zhong[3], Jie Huang[3], Hao Sun[3], Ming-Ying Zheng[3], Fa-Man Xiao[3], Hong-Hong Yan[3], Dan-Xia Lu[3], Zhi-Yi Lv[3], Yi-Long Wu[3], Hua-Jun Chen[3], Jin-Ji Yang[1,2,3]

[1]Guangdong Lung Cancer Institute, Guangdong Provincial People's Hospital (Guangdong Academy of Medical Sciences), Southern Medical University, Guangzhou, China; [2]School of Medicine, South China University of Technology, Guangzhou, China; [3]Guangdong Lung Cancer Institute, Guangdong Provincial People's Hospital, Guangdong Academy of Medical Sciences, Guangzhou, China; [4]Department of Pathology, Guangdong Provincial People's Hospital, Guangdong Academy of Medical Sciences, Guangzhou, China

Contributions: (I) Conception and design: HJ Chen, JJ Yang; (II) Administrative support: HJ Chen, JJ Yang; (III) Provision of study materials or patients: All authors; (IV) Collection and assembly of data: SL Zhang, CY Zhang, YQ Chen; (V) Data analysis and interpretation: All authors; (VI) Manuscript writing: All authors; (VII) Final approval of manuscript: All authors.

[#]These authors contributed equally to this work.

Correspondence to: Hua-Jun Chen, MD. Guangdong Lung Cancer Institute, Guangdong Provincial People's Hospital, Guangdong Academy of Medical Sciences, 106 Zhongshan 2nd Road, Guangzhou 510080, China. Email: chenhuajun@gdph.org.cn; Jin-Ji Yang, MD. Guangdong Lung Cancer Institute, Guangdong Provincial People's Hospital (Guangdong Academy of Medical Sciences), Southern Medical University, Guangzhou, China; School of Medicine, South China University of Technology, Guangzhou, China; Guangdong Lung Cancer Institute, Guangdong Provincial People's Hospital, Guangdong Academy of Medical Sciences, 106 Zhongshan 2nd Road, Guangzhou 510080, China. Email: yangjinji@gdph.org.cn.

Background: The transformation of epidermal growth factor receptor (*EGFR*)-mutant lung adenocarcinoma (LUAD) into small cell lung cancer (SCLC) accounts for 3–14% of the resistance mechanism to EGFR tyrosine kinase inhibitors (TKIs). At present, there is no relevant research to explore the dynamic expression of *EGFR*-mutant proteins and genomic evolution in *EGFR*-mutant transformed SCLC/neuroendocrine carcinoma (NEC).

Methods: Genetic analysis and protein level analysis by next-generation sequencing (NGS), Whole-exome sequencing (WES) and immunohistochemistry were performed to explore expression of *EGFR*-mutant proteins and genomic evolution in *EGFR*-mutant transformed SCLC. The research used three patient-derived organoids (PDOs) to explore the efficacy of combo [chemotherapy (chemo) plus TKI or bevacizumab] treatment. According to the subsequent treatment regimens after SCLC/NEC transformation, 35 patients were divided into chemo (n=21) and combo (n=14) groups.

Results: *EGFR* L858R and *EGFR* E746–750 del protein expression by immunohistochemistry was 80.0% (4/5) and 100% (6/6), respectively (P=0.455) in initially-transformed tissues. Meanwhile, *EGFR*-mutant proteins were expressed in 85.7% (6/7) of dynamic rebiopsy tissues or effusion samples after the first transformation. Then, by the pathway enrichment analysis of tissue and plasma NGS, the EGFR-related pathways were still activated after SCLC/NEC transformation. Moreover, WES analysis revealed that transformed SCLC shared a common clonal origin from the baseline LUAD. The drug sensitivity of three PDOs demonstrated potent anti-cancer activity of EGFR-TKIs plus chemo, compared with chemo or TKI alone. There were significant differences in objective response rate (ORR) between the combo and chemo groups [42.9 % *vs.* 4.8%, P=0.010, 95% confidence interval (CI): 1.5–145.2]. Furthermore, the median post-transformation progression-free survival (pPFS) was significantly prolonged in the combo group, with 5.4 (95% CI: 3.4–7.4) versus 3.5 (95% CI: 2.7–4.3, P=0.012) months.

Conclusions: *EGFR* 19del or L858R-mutant proteins could be constantly expressed, and EGFR pathway still existed in *EGFR*-mutant transformed SCLC/NEC with a common clonal origin from the baseline LUAD. Taking together, these molecular characteristics potentially favored clinical efficacy in transformed

SCLC/NEC treated with the combo regimen.

Keywords: Epidermal growth factor receptor-mutant proteins (*EGFR*-mutant proteins); genomic evolution; resistance; small cell lung cancer (SCLC); histologic transformation

Submitted Jan 31, 2023. Accepted for publication Jul 28, 2023. Published online Sep 04, 2023.
doi: 10.21037/jtd-23-161
View this article at: https://dx.doi.org/10.21037/jtd-23-161

Introduction

Compared with the traditional treatment, epidermal growth factor receptor (EGFR) tyrosine kinase inhibitors (TKIs) have significantly improved the clinical outcomes for advanced non-small cell lung cancer (NSCLC) harboring EGFR-activating mutations (1-5). Currently, the mechanism of acquired resistance is known to include second-site *EGFR* mutations (e.g., the T790M mutation) (6), bypass activation [such as *MET* (7) and *Her2* amplification (8)], and histological transformation, but it still needs to be further elucidated. Small cell lung cancer (SCLC) transformation is one of the most frequent pathological types in histological transformation, reported in 3–14% of resistant cases (9,10). Besides the EGFR-TKI resistance, the transformation from NSCLC to SCLC was also reported in patients receiving immune checkpoint inhibitors (11-13) and anaplastic lymphoma kinase (ALK)-TKIs (14-17) as one of the mechanisms of acquired resistance.

The mechanisms of transformation from NSCLC to SCLC remain controversial. One of the hypotheses is that lung adenocarcinoma (LUAD) and SCLC have a common cell origin (18). Previous study has shown that the cell of origin of SCLC could arise undifferentiated precursor cells (19). In addition, tumor arising from neuroendocrine cells is carcinoid (20), and Baine *et al.* (21) pointed that POU2F3 was expressed in 75% of SCLC with entirely negative or minimal neuroendocrine marker expression. So the cell of origin of SCLC has not been formally identified. However, our study focused on the research of transformed SCLC. Several studies have indicated that the incidence of SCLC transformation has increased since EGFR-TKI has been used to treat LUAD (22,23). Furthermore, type II alveolar epithelial cells have been proven to have the potential to differentiate SCLC from LUAD. Importantly, most of the transformed SCLC still retains the *EGFR* mutation derived from NSCLC (9,24), indicating that the transformed SCLC is not an independent cancer species. In addition, another hypothesis is that the initial pathology is a mixture of LUAD and SCLC components (25), and subsequently, the SCLC component is dominant as the pathological type of LUAD is suppressed by EGFR-TKIs. In response to this hypothesis of mixed types, some scholars rejected the possibility of initially-mixed NSCLC and SCLC because many patients had previously received EGFR-TKI treatment and obtained a longer progression-free survival (PFS) (18). Due to the small biopsy histological samples, the coexistence of NSCLC and SCLC at the time of initial diagnosis cannot be excluded (24,26).

The most common resistance mechanism is the T790M mutation, and SCLC transformation is rarely reported in the published literature. Furthermore, there is no consensus on the treatment of transformed SCLC, and chemotherapy (chemo)

Highlight box

Key findings

- Epidermal growth factor receptor (*EGFR*)-mutant proteins could be constantly expressed, and EGFR pathway still existed in *EGFR*-mutant transformed small cell lung cancer (SCLC)/neuroendocrine carcinoma with a common clonal origin from the baseline lung adenocarcinoma.

What is known and what is new?

- Previous research has shown that platinum-etoposide was the most commonly used treatment after SCLC conversion, and the median progression-free survival was only 3.5 months.
- At present, there is no relevant research to explore the dynamic expression of *EGFR*-mutant proteins in *EGFR*-mutant transformed SCLC.
- Our study demonstrated that the combo regimen (chemotherapy plus EGFR-tyrosine kinase inhibitors or bevacizumab) could improve the efficacy in transformed SCLC. Our paper also demonstrated *EGFR*-mutant proteins could be constantly expressed in *EGFR*-mutant transformed SCLC.

What is the implication, and what should change now?

- The combo regimen could improve the clinical efficacy in *EGFR*-mutant transformed SCLC. However, the mechanism of the combined regimen still needs to be further explored by multicenter clinical studies with larger sample sizes.

alone is usually administered to overcome such resistance. However, previous research has shown that the median PFS of chemo alone was only 3.4 months [95% confidence interval (CI): 2.4 to 5.4] with the platinum-etoposide, and 2.7 months (95% CI: 1.3 to 3.4) with taxanes (27). Platinum-etoposide was the most commonly used treatment after SCLC conversion, and the median PFS was only 3.5 months (28).

Previous studies have confirmed that patients with triple mutations are more likely to undergo SCLC transformation. At the genetic level, pathways related to transformation include *RB1*, *PTEN*, and *SOX* (23,29-32). At present, there has been no relevant research to explore the dynamic expression of *EGFR*-mutant proteins in *EGFR*-mutant transformed SCLC. Here, we retrospectively describe the expression of *EGFR*-mutant proteins and genomic evolution in *EGFR*-mutant transformed SCLC. We present this article in accordance with the MDAR reporting checklist (available at https://jtd.amegroups.com/article/view/10.21037/jtd-23-161/rc).

Methods

Patients and data extraction

We retrospectively analyzed advanced *EGFR*-mutant LUAD patients from Guangdong Provincial People's Hospital from January 2010 to September 2020 who were treated with EGFR-TKIs and underwent a transformation into SCLC or neuroendocrine carcinoma (NEC)—hereinafter collectively referred to as SCLC transformation. All patients with acquired drug resistance underwent rebiopsy to confirm transformation to SCLC or NEC. In this study, we defined incomplete SCLC transformation as pathologically confirmed SCLC combined LUAD components. We defined the term NEC as pathologically confirmed high-grade NECs. The study was conducted in accordance with the Declaration of Helsinki (as revised in 2013). Ethical approval was obtained from the Ethical Review Committee of Guangdong Provincial People's Hospital [No. GDREC2019217H(R1)]. Furthermore, written informed consent was obtained from the patients or their immediate family members. The last follow-up time was on September 30, 2022.

Pathology and imaging

Tissue and pleural effusion sediment were fixed in 4% formaldehyde, and 3-μm sections were stained with hematoxylin and eosin (HE) reagent after being embedded in paraffin, and then examined with a Nikon 80i microscope (×200 magnification).

Immunohistochemistry (IHC) was done with the tissue and pleural effusion sediment staining fixed in 4% paraformaldehyde and embedded in paraffin. Sections of 3 μm were prepared, and immunohistochemical staining of cytokeratin 7 (CK7), thyroid transcription factor 1 (TTF1), chromogranin A (CgA), synaptophysin (Syn), CD56, Napsin A, and Ki67 were conducted. Each section was examined under a ×200 power field. Positive cells were scored as expressing <10% (–), 10% to 25% (+), >25% to 75% (++), and >75% (+++).

EGFR-mutant protein expression by IHC

We used *EGFR* exon 19 deletion (19del) (E746-A750del Specific) (6B6) XP® Rabbit monoclonal antibody (mAb) (Cell Signaling Technology, Danvers, MA, USA) and EGF Receptor (L858R mutant specific) (43B2) rabbit mAb (Cell Signaling Technology) to detect EGFR expression when first transforming tissues. Before performing the IHC assay for EGFR protein expression, the patients' samples were tested for next-generation sequencing (NGS) or amplification refractory mutation system (ARMS). The criteria for evaluating protein expression were staining intensity which was assessed from "–" (complete absence of staining or faint staining intensity in <10% cells) to "+++" (tumor cells had strong staining) (33).

NGS analysis of tissue and liquid biopsy samples

Tissue and liquid biopsy samples for NGS analysis were sent to two laboratories, including Burning Rock Biotech and Nanjing Geneseeq Technology Inc., (Nanjing, China), which were also accredited by the College of American Pathologists and certified by the Clinical Laboratory Improvement Amendments. According to a previous study (34), the samples were processed using protocols from the Burning Rock Biotech. NGS was performed in the Burning Rock Biotech using Nextseq 500 (Illumina) platform. Besides, we used 168 lung cancer-relevant gene panels or at most 520 lung cancer-relevant gene panels to capture targeted genes. Then, at Nanjing Geneseeq Technology Inc., NGS was performed on a HiSeq 4000 (Illumina) platform, which capture-based targeted NGS of 425 lung cancer-related genes. At Nanjing Geneseeq Technology Inc., experimental operation and data analysis were performed as described in

the literature (35).

Whole-exome sequencing (WES) of tissue biopsy samples

DNA was extracted from thick serial sections cut from tumor tissue samples and control sections. In addition, we performed DNA extraction from the formalin-fixed paraffin-embedded (FFPE) by the DNeasy Blood and Tissue Kit (69504, QIAGEN, Venlo, Netherlands).

Targeted capture pulldown and exon-wide libraries were built with previously extracted DNA using the xGen® Exome Research Panel (Integrated DNA Technologies, Inc., Skokie, Illinois, USA) and TruePrep DNA Library Prep Kit V2 for Illumina (#TD501, V azyme, Nanjing, China). Paired-end sequencing was performed on NovaSeq 6000 System (Illumina, Inc.) with an average sequencing depth of 150× for controls and 320× for tumor tissues.

The sequence data were aligned to the human reference genome (NCBI build 37) using Burrows-Wheeler Aligner (BWA), and Binary Alignment Map (BAM) data was processed using sambamba. Somatic mutations identification and indels were processed using Mutect and Somatic Indel Detector software. Genes were annotated using ANNOVAR, and then converted to a mutation annotation format (MAF) file through the map tool. The landscape of the top driver mutation spectrum was visualized via R Script, including mutation.

The tumor mutation burden (TMB) of a tumor sample is determined by the number of non-synonymous somatic mutations (single nucleotide variants and small insertions/deletions) per mega-base in coding regions, and it reflects the amount of coding errors of all mutation events. Somatic copy number variants (CNVs) in tumor-normal samples were detected using the facets package.

Clonal evolution analysis

Variant allele frequency, the copy number of the genomic region containing the mutation, and an estimate of tumor content were used to input the cyclone. Then the proportion of cell clones with a specific mutation (cellular prevalence) was calculated. The optimal tree solutions were obtained with the iterative version of the setup. Then, each patient's fish plot and phylogenetic tree were depicted with a timescape (36).

Specimen preparation and culture of patient-derived organoid (PDO)

Lung cancer organoids (LCOs) were mainly derived from malignant serous effusion (MSE) and tissue specimens. In general, MSE was obtained by thoracentesis, placed in a sterile bag containing heparin (10 U/mL), and transported to the laboratory at low temperature (2–8 ℃) within 4 h. Then, the sample was centrifuged at 300 g for 5 min at 4 ℃, and the cell pellet was resuspended in Accuroid® in lung cancer media (ALCM, Accurate International Biotechnology Co., Guangzhou, China). As for tissue specimens, the cultivation method was demonstrated in a previous study (37). The isolated tumor tissue was divided into 1 mm^3 fragments and separated into cold Hank's balanced salt solution (HBSS) with antibiotics (Lonza, Basel, Switzerland) and transported to the laboratory on ice within 1 h after removal from the patient. After washing three times with cold HBSS containing antibiotics and sectioning with sterile blades, the samples were incubated with 0.001% DNase (Sigma-Aldrich, MO, USA), 1 mg/mL collagenase/dispase (Roche, IN, USA), 200 U/mL penicillin, 200 mg/mL streptomycin, and 0.5 mg/mL amphotericin B (2% antibiotics, Sigma) in DMEM/F12 medium (Lonza) at 37 ℃ for 3 h with gentle agitation and intermittent resuspension. After that, the digested tissue suspension was repeatedly triturated via pipetting and passed through a 70-μm filter.

The cell suspension produced from MSE or tissues was centrifuged at 112 rcf for 3 min. Then, the pellet was resuspended in ALCM. After that, 200 μL Matrigel (Corning, New York, NY, USA) was added to 100 μL of the cell suspension for establishing organoids, and the resulting suspension was allowed to solidify on pre-warmed 6-well culture plates (Corning) at 37 ℃ for 30 min. After gelation, 3 mL minimum basal medium (MBM) was added to each well. The medium was changed every 2–3 days.

Drug sensitivity testing

Organoids cultured over 2 weeks were harvested and dissociated using 1× TrypLe (Gibco, Waltham, MA, USA). The dissociated organoids were mixed in MBM + Matrigel (1:3 ratio) and seeded onto 384-well white plates. After gelation, 30-μL MBM was added to each well. The organoids were cultured for 48 h. After that, a dilution series of each compound (50, 10, 2, 0.4, 0.08, and 0.016 μM) was dispensed using liquid-handling robotics, and cell viability was assayed using CellTiter-Glo (Promega, Madison, WI, USA) after 4 days of drug incubation. The plates were agitated for 30 min at room temperature prior to measuring luminescence. Half-maximal inhibitory concentration (IC50) values were determined using GraphPad Prism 7.0

(GraphPad Software, La Jolla, CA, USA).

Statistical analysis

In our study, the PFS of a certain treatment was defined as the period from the initial date of the treatment to radiologically-confirmed disease progression or death. The post-transformation progression-free survival (pPFS) of the subsequent regimen was referred to the time from transformation to disease progression or death. The post-transformation overall survival (pOS) was defined as the period from the date of pathologically confirmed transformation until death or the last follow-up and objective response rate (ORR) was defined as the proportion of complete response (CR) or partial response (PR).

We defined the time to transformation (TTT) as the time from the initial pathology diagnosis of locally-advanced or metastatic (stage IIIB without any indications for curative chemoradiation or other local treatments to stage IV) LUAD to the additional biopsy revealing the metachronous SCLC/NEC phenotype.

In all statistical analyses, R statistical software (version 3.6.1; Vienna, Austria) was used. Two groups' baseline characteristics and odds ratio (OR) were compared using the χ^2 test or Fisher's exact test. Survival analyses were constructed with the Kaplan-Meier method, and differences were estimated by a log-rank test. Several clinically relevant factors (smoke, pathology, stage, brain metastasis, *EGFR* mutation) were entered into a multivariate Cox proportional hazards model. Two-sided P values <0.05 were considered statistically significant.

Results

Clinical efficacy of chemo and combo (chemo plus TKI or bevacizumab) groups in transformed SCLC/NEC

The study screened 1,441 patients from January 2010 to September 2020, and 49 transformed SCLC/NEC patients were included in our study. Then, 14 patients were excluded, including seven who were lost to follow-up and seven more who received other treatments (e.g., only EGFR-TKIs, best supportive care, immunotherapy plus chemo) (Figure S1). The clinical characteristics and the clinicopathologic characteristics are summarized in Tables S1,S2.

In total, 35 transformed SCLC/NEC patients were eligible for the final analyses. According to the subsequent treatment regimen just after SCLC transformation, patients were divided into 21 with only chemo (chemo group) and 14 with chemo plus bevacizumab or EGFR-TKIs (combo group). There were significant differences in ORR between the chemo and combo groups (4.8% *vs.* 42.9%, P=0.010, 95% CI: 1.5–145.2) (*Figure 1A*). Finally, the median pPFS was also significantly prolonged in the combo group [5.4 (95% CI: 3.4–7.4) versus 3.5 (95% CI: 2.7–4.3) months, P=0.012] (*Figure 1B*). However, there was no significant difference in the median pOS between the two groups [10.7 (95% CI: 5.6–15.8) versus 7.7 (95% CI: 5.2–10.2) months, P=0.377] (*Figure 1C*).

EGFR-mutant proteins were expressed in complete or incomplete transformed SCLC at the initial transformation

In our study, IHC data were gathered for 11 patients of a total of 35 patients with sufficient tissues after transformation. The information of 11 patients could be seen in Table S3. The IHC of *EGFR* 19del (E746-A750del) protein and L858R protein was conducted in six and five patients, respectively. The expression of the mutated protein was 100.0% (6/6) for 19del and 80.0% (4/5) for L858R mutation. Besides, with respect to the expression of mutated protein, the combo group, and chemo group respectively accounted for 87.5% (7/8) and 100.0% (3/3) (P=1.00). However, 11 patients responded to the combo treatment or chemo alone (*Figure 2* and Figure S2). Among six patients (three combined and pure SCLC patients respectively) harboring the *EGFR* 19del, *EGFR* 19del protein expression was positive in P8 with complete SCLC transformation, and this patient achieved a pPFS of 5.1 months treated with the combo regimen (*Figure 2A*). P9 with incomplete SCLC transformation was also positive in *EGFR* 19del expression and achieved a pPFS of 8.9 months with the combo regimen. In terms of the expression of *EGFR* L858R, P15 with transformed-NEC and weakly positive *EGFR* L858R achieved a pPFS of 6.1 months after irinotecan-cisplatin (IP) chemo (*Figure 2B*).

Notably, P13, which developed concomitant resistance mechanisms of SCLC transformation and T790M mutation after first-line erlotinib, was similar to several case reports of dual resistance mechanisms (38-40). After transformation, the L858R protein was still positive. P13 achieved PR and a PFS of 10.0 months with osimertinib plus IP (Figure S2).

EGFR-mutant protein expression among the two groups revealed the genotypic complexity of transformed SCLC/NEC.

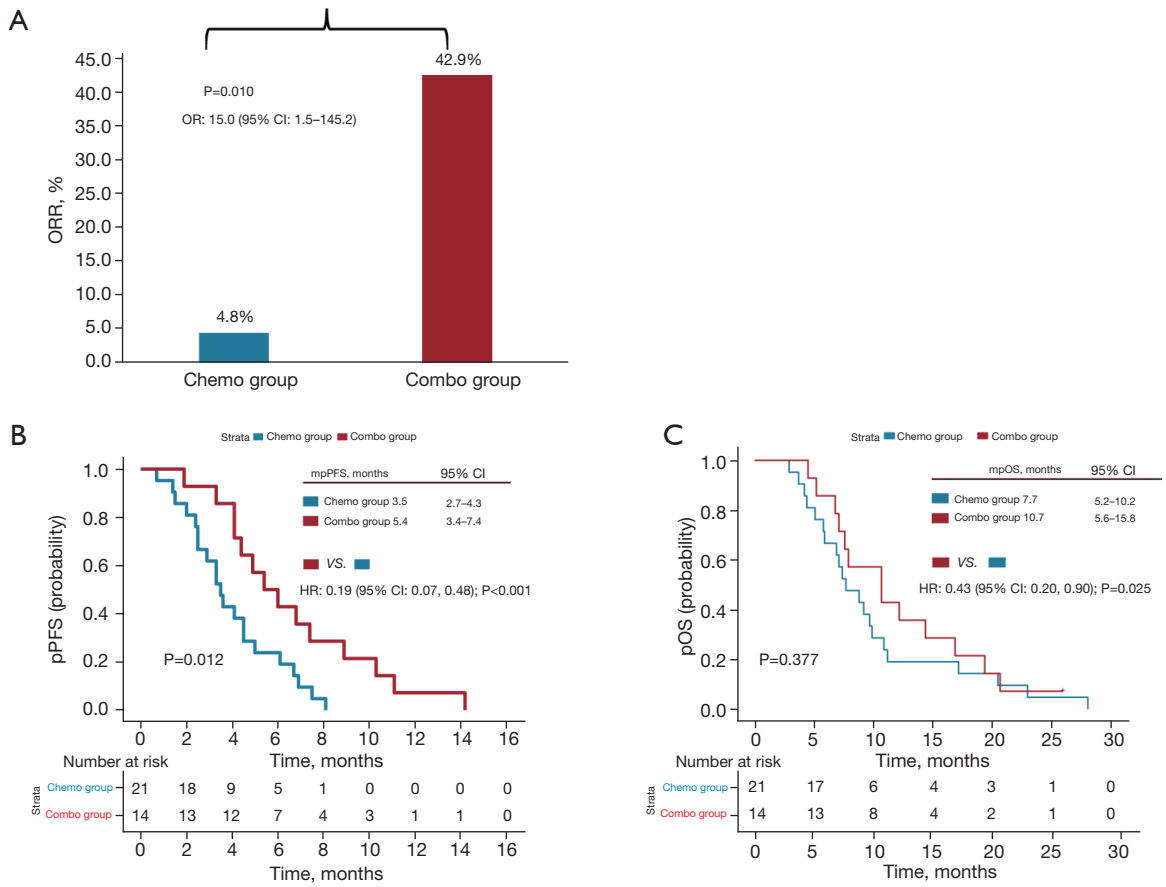

Figure 1 The efficacy of subsequent treatment in transformed *EGFR*-mutant SCLC/NEC. (A-C) Kaplan-Meier curves illustrate the pPFS (B) and pOS (C) of the patients who received combo therapy (red) and chemo (blue). ORR, objective response rate; OR, odds ratio; CI, confidence interval; chemo, chemotherapy; combo, chemo plus TKI or bevacizumab; TKI, tyrosine kinase inhibitor; mpPFS, median post-transformation progression-free survival; HR, hazard ratio; mpOS, median post-transformation overall survival; EGFR, epidermal growth factor receptor; SCLC, small cell lung cancer; NEC, neuroendocrine carcinoma.

Dynamic expression status of EGFR-mutant proteins and tumor marker changes after initial transformation

In our study, we performed IHC of the *EGFR*-mutant proteins 19del (E746–750) and L858R on four patients with sufficient serial samples after initial transformation (*Figure 3*). Meanwhile, this study dynamically monitored the changes of carcinoembryonic antigen (CEA) and neuron-specific enolase (NSE) in plasma of four patients. Firstly, the frequency of *EGFR*-mutant proteins was 85.7% (6/7) in the serial samples after transformation. However, 19del protein was not expressed in the paravertebral tissue of P8 at the last biopsy. Secondly, in the combo group, CEA change of P8 patient was relatively stable while NSE decreased significantly with treatment. However, NSE increased significantly in progressive disease (PD). In P9 patient, CEA increased significantly in PD, while NSE remained relatively stable. Finally, in the chemo group, CEA change of P20 patient was relatively stable while NSE decreased significantly with treatment. However, NSE increased significantly in PD. In P19 patient, CEA increased significantly in PD, while NSE remained decreased.

Transformed SCLC may share a common clonal origin from the baseline LUAD

The results of the clonal evolution diagram indicated that the main clones of baseline LUAD were different from those after transformation to SCLC/combined SCLC with LUAD. In P7, the LUAD was mainly composed of clones

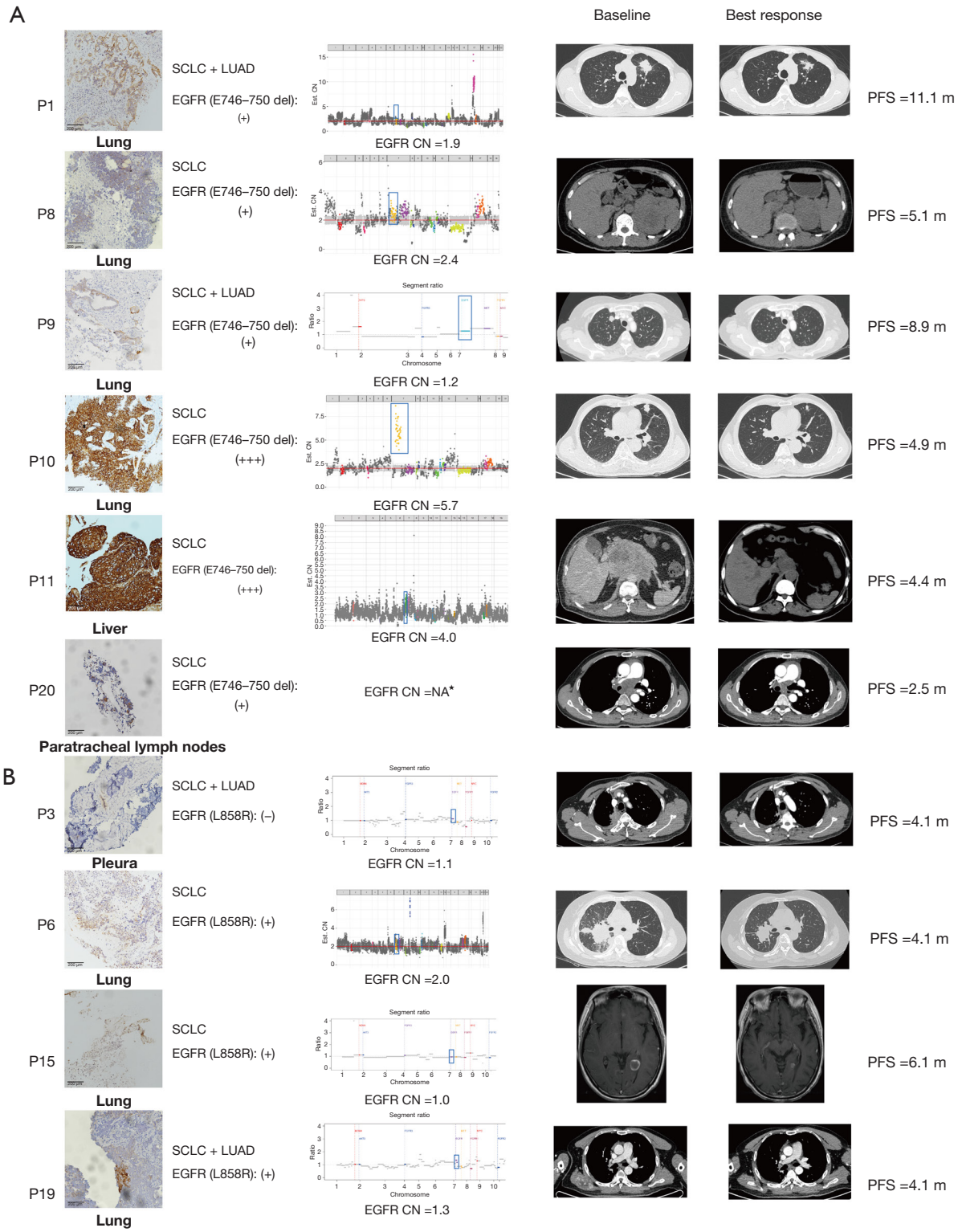

Figure 2 Expression status of *EGFR*-mutant proteins of ten patients at initial transformation and their treatment response. The status of targeted lesions at initial transformation and the best response of the combo therapy or chemotherapy was evaluated by computed tomography scan. The percentages of tumor shrinkage (–) or enlargement (+) were indicated beside the investigator-assessed objective

response evaluated based on RECIST 1.1. (A) IHC results (magnification, ×200) of six samples after first transformation with *EGFR* exon 19 E746–750 del. Two of 5 patients showed strongly positive (+++) of mutant EGFR protein expression, whereas others showed weakly positive expression. (B) IHC results (magnification, ×200) of four samples when initially transformed with *EGFR* L858R mutation. Three of 4 patients showed weakly positive (+) mutant EGFR protein expression. –, complete absence of staining or faint staining intensity in <10%; +, >10% tumor cells had faint staining; +++, tumor cells had strong staining. *, the patient has not enough tissues to perform NGS. P, patient; SCLC, small cell lung cancer; LUAD, lung adenocarcinoma; EGFR, epidermal growth factor receptor; del, deletion; Est., estimated; CN, copy number; PFS, progression-free survival; m, months; NGS, next-generation sequencing; NEC, neuroendocrine carcinoma; RECIST 1.1, response evaluation criteria in solid tumors guidelines (version 1.1); IHC, immunohistochemistry.

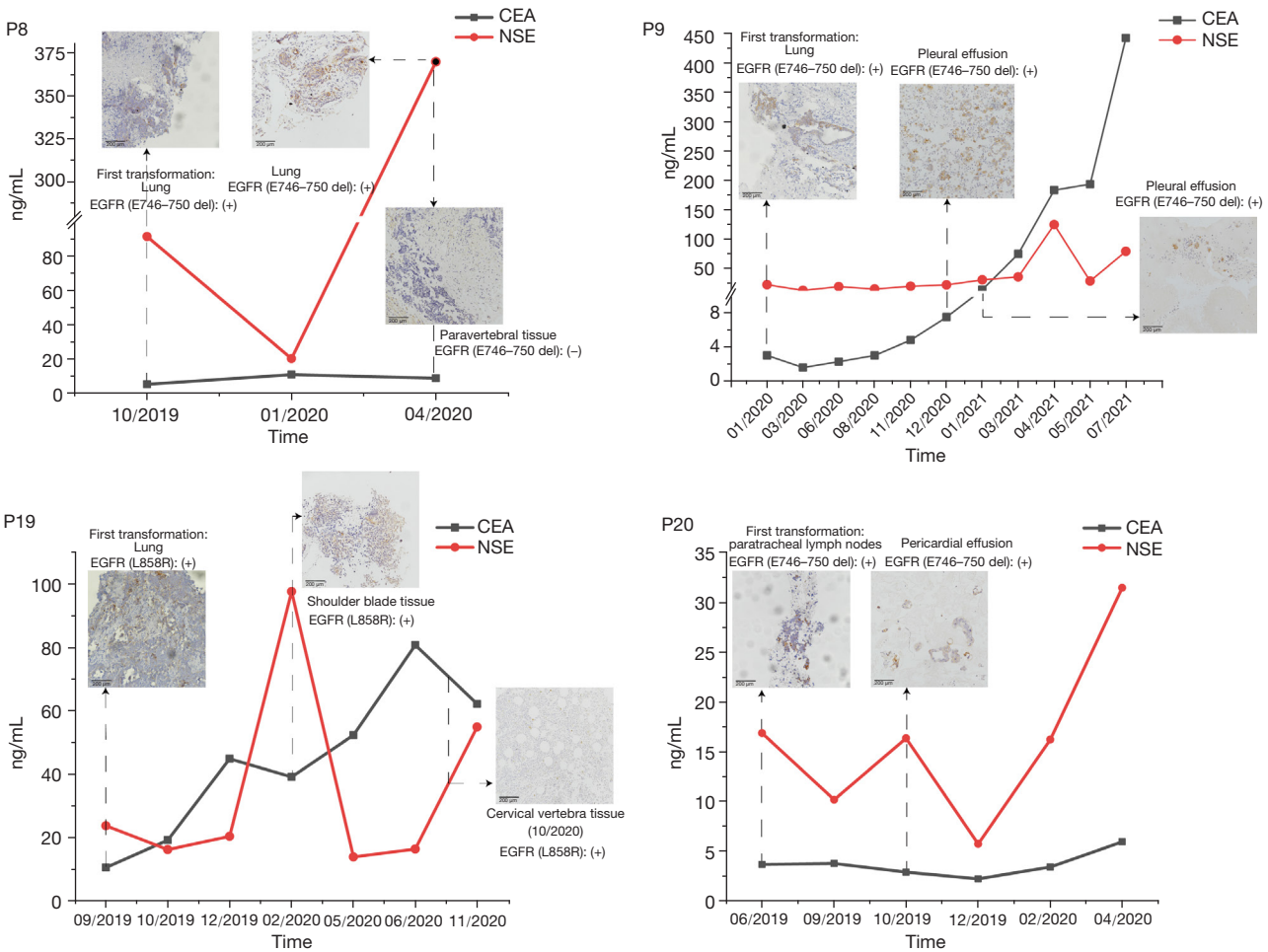

Figure 3 Dynamic expression status of *EGFR*-mutant proteins (IHC; magnification, ×200) and tumor marker changes after initial transformation. CEA and NSE were observed in four patients after the initial transformation. EGFR, epidermal growth factor receptor; del, deletion; CEA, carcinoembryonic antigen; NSE, neuron-specific enolase; IHC, immunohistochemistry.

0, 4, 5, and 6, while the transformed SCLC combined with LUAD was mainly composed of clones 1, 2, and 5 (*Figure 4A*). In P11, the LUAD was mainly composed of clones 0, 2, and 7, while the transformed SCLC was mainly composed of clones 0, 2, 3, and 4 in the retroperitoneal lymph node and 0, 3, 4, 5 in the liver (*Figure 4A*). According to the results of primary clones, the primary clones of the two patients after transformation were not directly derived from the primary clone of baseline LUAD but possibly from the same clone. Meanwhile, clone clustering

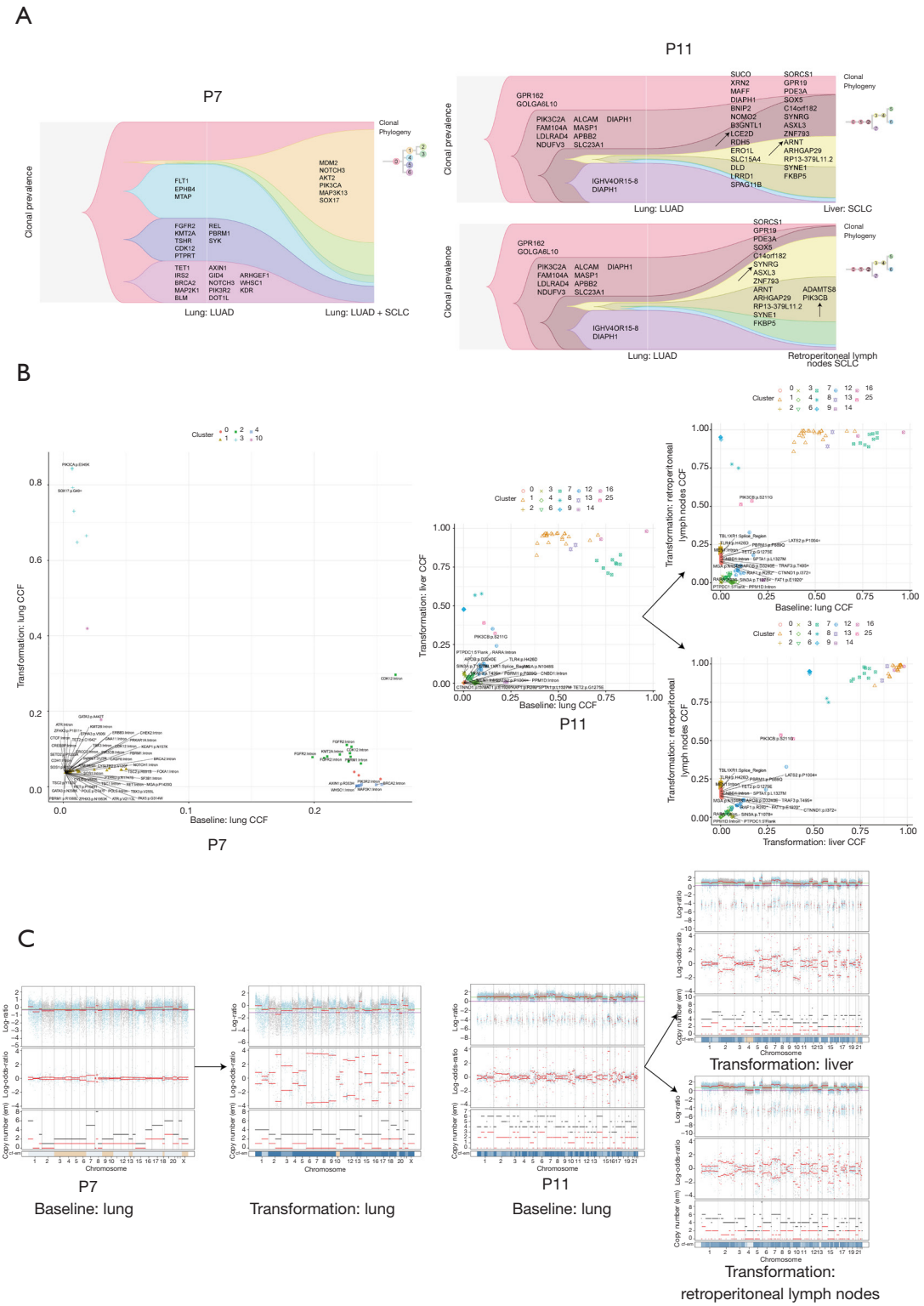

Figure 4 Clonal evolution analysis, subclones analysis, and genome stability by WES. (A) Two patients' fish plots were established by timescape. Different clones are used in different colors. Genes of each clone are shown in the fish plots. (B) Two patients' clonal cluster analysis. The predicted CCF distributions for each cluster are plotted. Clusters are annotated with gene mutation. (C) Facets analysis. The

top panel displays the total copy number logR, and the second panel displays allele-specific logOR with chromosomes alternating in blue and gray. Beige color is used to describe normal diploid (total =2, minor =1). The third panel plots the corresponding integer (total copy number used by black color to describe, minor copy number used by red color) copy number calls. The estimated cf profile reveals clonal and subclonal copy number events. P, patients; LUAD, lung adenocarcinoma; SCLC, small cell lung cancer; CCF, cancer cell fraction; cf, cellular fraction; WES, whole-exome sequencing; logR, log-ratio; logOR, log-odds-ratio.

of P7 and P11 was performed (*Figure 4B*), indicating that transformed SCLC may share a common clonal origin with baseline LUAD. Facet analysis (41) showed that the genomic instability of P7 increased after transformation, while the genomic instability of P11 changed little (*Figure 4C*). This might indicate that the combo regimen was less efficacious in P7 than in P11 (Table S2). According to heat-map analysis, both P7 and P11 retained some genes of LUAD after transformation, such as *TP53* mutation after transformation in P7 and *EGFR* mutation and *TP53* frameshift mutation after transformation in P11. However, both had specific gene mutations after transformation, such as *MGA*, *PBRM1*, and *APOB* mutation in P11 (Figure S3A). TMB tests were performed on the baseline and transformed tissues of both patients. Compared with baseline, TMB increased in both patients after transformation (Figure S3B). The mutation spectrum was also significantly altered in both patients after transformation, and the median ratio mutation spectrum of C>A in P7 and P11 significantly increased after transformation (Figure S3C).

The EGFR pathways were present in transformed SCLC/NEC

In this study, the paired tissues in seven patients at baseline and the initial SCLC/NEC transformation were eligible for the NGS. Among them, the pathological diagnosis of P1 after initial transformation was combined SCLC with LUAD, and combined SCLC with NEC in P14. The analysis of genomic profiles of seven patients revealed that *EGFR* mutations remained all at the initial transformation. Meanwhile, *EGFR* mutations were also detected in the paired peripheral blood specimens of six patients. (*Figure 5A*). At the same time, there were also some differences in genetic profiles before and after transformation. For example, the *PIK3CA* mutation emerged in *P35* after transformation, which was related to the acquired resistance to EGFR-TKIs.

Besides, one patient (P19) underwent plasma genetic testing at three time points after the initial confirmed transformation (*Figure 5B*). Dynamic plasma genetic results showed that the patient retained the *EGFR* L858R mutation and *EGFR* T790M mutation although before and after chemo regimen. Meanwhile, the patient had *TP53* del and *RB1* mutation.

At the initial transformation, four patients (P1, 5, 8, and 14) in our study underwent a second NGS analysis using peripheral blood samples during the follow-up. The pathway enrichment analysis of NGS was performed on both tissues and peripheral blood samples at the initial transformation, as well as on peripheral blood samples at the second-time follow-up just after the initial transformation. The results showed that the pathways were enriched in *ERB2*, *RAS*, *PI3K-AKT*, and *mTOR* (*Figure 5C*), all related to the EGFR signaling pathway (42). Based on the above results (*Figure 5*), the EGFR pathway still existed in transformed SCLC/NEC, both in the Combo and the chemo groups.

PDO preliminarily validated the efficacy of combo regimens in transformed SCLC/NEC

To establish a reliable preclinical model that can faithfully reflect the biological characteristics of transformed SCLC, we cultivated three-dimensional (3D) organ models derived from tissue or MSE. SCLC transformation occurred in all three patients after EGFR-TKIs resistance. Drug-resistant tumor tissue and effusion samples were collected from each patient. Fresh tumor specimens were derived from pleural or lung biopsy. The processed cell suspension was obtained, and after culturing for two to three weeks, 3D organoid models were gradually established (*Figure 6*). Due to the limitation of specimens, only one case (P17) of PDO in three cases was histologically validated as NEC (*Figure 6A*). The IHC of the patient's pleural effusion resulted as Syn (+), CD56 (++), and CgA (weakly +). At the same time, the IHC of LCOs derived from this sample showed consistent results [Syn (+), CD56 (+), CgA (+)]. Whether *in vivo* or *in vitro*, tumors diagnosed as neuroendocrine tend to be SCLC. To evaluate the drug response of PDO, we formulated several programs according to the patient's pathological type and genetic mutation, including targeted and chemo drugs or

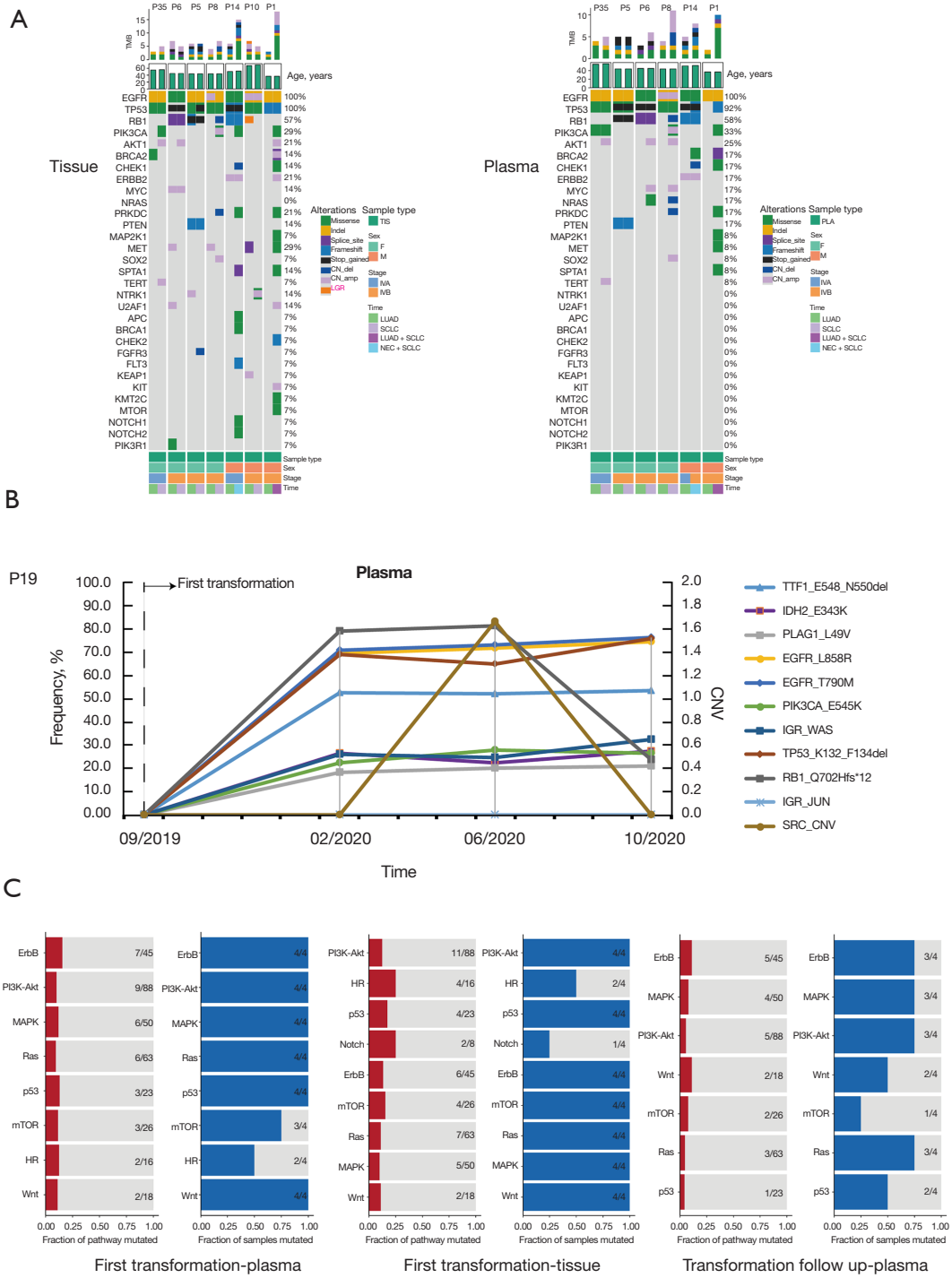

Figure 5 Genomic evolution and molecular signaling pathway enrichment. (A) Genetic profiles of LUAD and transformed SCLC or NEC tissues were matched in seven patients. Then, genetic profiles of LUAD and transformed SCLC or NEC plasma were matched in six patients. (B) Dynamic changes of plasma gene in one patient after the first transformation. (C) The signaling pathways were enriched in four patients' plasma and tissues of the first transformation and the transformed follow-up samples. In the left-most red bar, 7/45 means that 45 gene variants related to the ErbB pathway were detected at a detection level of 168 panels, and a total of 7 gene variants were enriched in the ErbB pathway in 4 patients. In the blue bar chart, for example, 3/4 means that 3 out of 4 patients have associated gene variants enriched in the mTOR pathway. The data meaning in other graphs is the same as above. TMB, tumor mutation burden; P, patients; EGFR, epidermal growth factor receptor; CN, copy number; del, deletion; amp, amplification; LGR, large genomic rearrangement; TIS, tissue; PLA, plasma; LUAD, lung adenocarcinoma; SCLC, small cell lung cancer; NEC, neuroendocrine carcinoma; CNV, copy number variant.

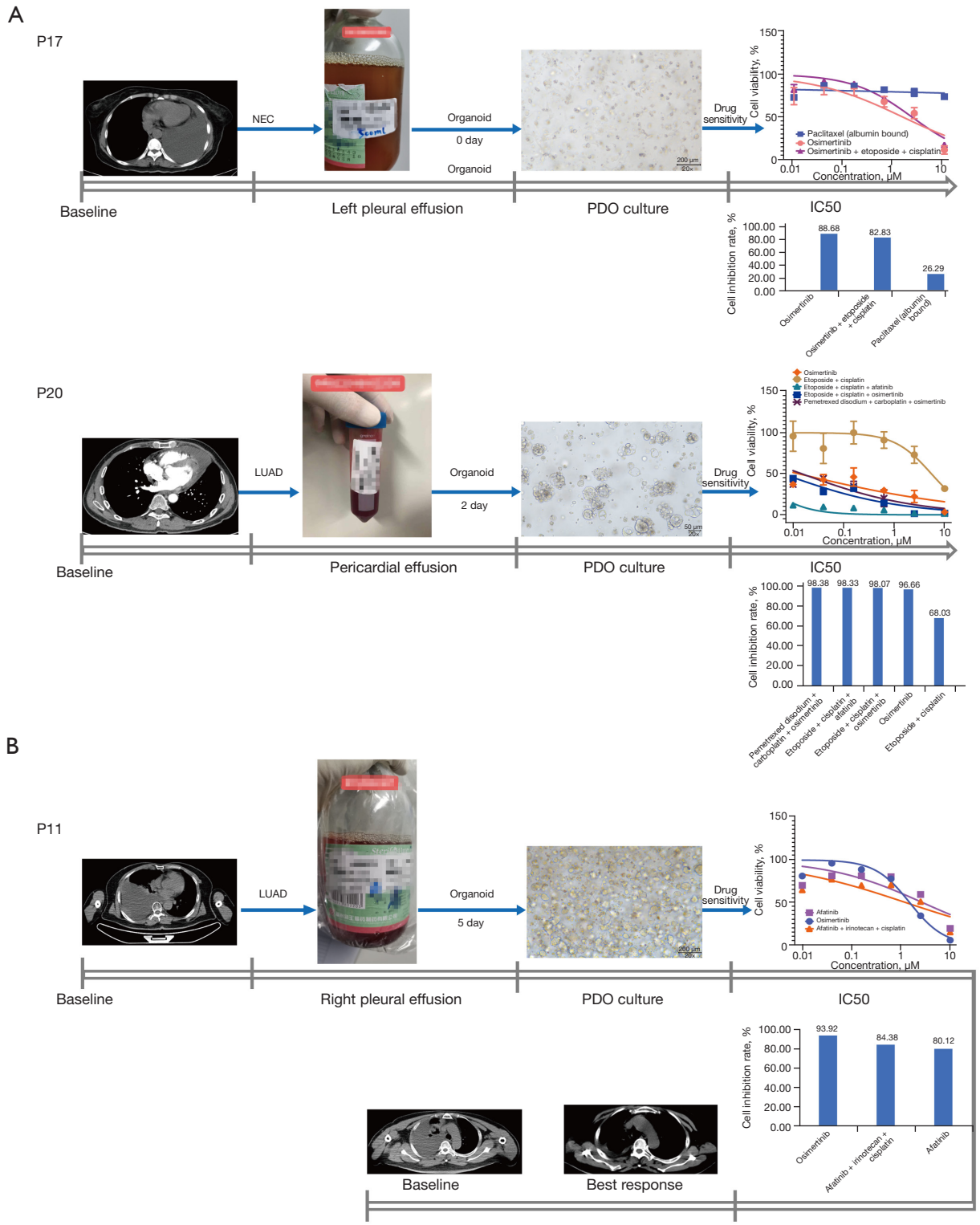

Figure 6 PDO drug sensitivity tests predict patients' clinical treatment response. (A) The PDOs were derived from pleural tissue, pericardial effusion. (B) Drug sensitivity test of 3D organoid and the clinical efficacy of a typical patient. P, patients; NEC, neuroendocrine carcinoma; PDO, patient-derived organoid; LUAD, lung adenocarcinoma; IC50, half-maximal inhibitory concentration; 3D, three-dimensional.

combo. The drug sensitivity of both patients displayed the most significant response to EGFR-TKIs combined with chemo. However, in clinical practice, drug-susceptibility tests of P11 showed that afatinib combined with chemo has a higher tumor inhibition rate (IC50 =1.26 μM) than the received afatinib plus IP and dramatically achieved PR after two cycles (*Figure 6B*). On the contrary, another patient (P20) received etoposide-cisplatin (EP) chemo alone, even though the drug susceptibility suggested that the EP regimen was resistant (IC50 =5.46 μM). As expected, non-target lesions had progressed rapidly after 2 months.

Discussion

Our study extensively investigated the expression of *EGFR*-mutant proteins and genomic evolution in *EGFR*-mutant transformed SCLC using *EGFR*-mutant protein expression, genomic landscape, and molecular signaling pathway enrichment. *EGFR*-mutant proteins were dynamically expressed in both LUAD and SCLC/NEC components. Transformed SCLC and LUAD shared genomic features of a common origin. Moreover, EGFR-related pathways still existed since the initial transformation. All these suggested better efficacy (ORR was 42.9% versus 4.8%, P=0.010, and median pPFS was 5.4 versus 3.5 months, P=0.012) in the combo group for SCLC-transformed patients with *EGFR* mutation after resistance to TKIs. *In vitro*, the drug sensitivity results of the PDOs also demonstrated potent anti-tumor activity of chemo plus EGFR-TKIs. To the best of our knowledge, this is the first retrospective study with a relatively large-sample size to potentially illustrate the molecular mechanism underlying the better efficacy of combo regimen in *EGFR*-mutant transformed SCLC/NEC.

IHC detected the *EGFR* 19del/L858R-mutant proteins not only in pure SCLC/NEC components but also in combined SCLC and LUAD components of transformed SCLC/NEC patients in our study. As far as we know, this is the first study using IHC to detect *EGFR* 19del/L858R-mutant proteins in dynamic samples after SCLC/NEC transformation. The results showed that the expression of *EGFR* 19del or L858R-mutant proteins was 90.9% (10/11) at the first transformation and 85.7% (6/7) in the serial samples. However, based on previous research, when *EGFR*-mutant lung cancer underwent SCLC transformation, the expression of *EGFR*-mutant proteins was lost (24). Besides, Li *et al.* (25) pointed that only LUAD components expressed *EGFR*-mutant protein in the combined SCLC. Meanwhile, the pathway enrichment analysis of plasma NGS revealed that the pathways were enriched in *ERB2*, *RAS*, *PI3K-AKT*, and *mTOR* (*Figure 5C*). When combined, the EGFR-related pathways were still activated after SCLC/NEC transformation, potentially indicating a better efficacy for SCLC/NEC-transformed patients treated with both EGFR-TKIs and chemo.

Unlike the study of Xie *et al.* (36)—which used pure transformed SCLC samples to explore the clonal evolution of transformed SCLC—we used partially-transformed tissues and transformed liver and retroperitoneal lymph nodes to investigate the clonal evolution of transformed SCLC. The similarities and differences in clonal evolution indicated that the main clones after transformation were not directly derived from the primary LUAD clones. However, the main clones might originate possibly from the same progenitor clone. This may provide a more comprehensive understanding of the evolution of transformed SCLC.

Better efficacy of EGFR-TKIs plus chemo in *EGFR*-mutant transformed SCLC/NEC was also observed in PDOs. The four PDOs of our study included histologically-confirmed pleural effusion with NEC, pericardial effusion with LUAD, pleural effusion with LUAD, and pleural tissue with NEC (*Figure 6* and Figure S4). The drug sensitivity of PDOs demonstrated potent anti-cancer activity of EGFR-TKIs plus chemo, compared with chemo or TKI alone. The successful cultivation of lung cancer 3D organoids was mainly focused on LUAD, LUSC, and SCLC in previous studies (43-45). However, this research did not include the organoid models of transformed SCLC. Therefore, this was the first application of PDOs to validate the efficacy of *EGFR*-TKIs plus chemo in *EGFR*-mutant transformed SCLC/NEC.

In our study, combo treatment was composed of chemo plus EGFR-TKIs and chemo (pemetrexed/carboplatin) plus bevacizumab, and two patients treated with the latter also achieved PR or stable disease (SD). On the other hand, only 11.4% (4/35) underwent a biopsy for more than two lesions at the time of transformation. Furthermore, 31.4% (11/35) had a subsequent rebiopsy. Therefore, multi-lesion and serial biopsy may help illustrate spatial and temporal histology heterogeneity of *EGFR*-mutant transformed SCLC/NEC, facilitating the final strategy of individualized treatment.

As a single-center study, the sample size was limited, and the retrospective study has a certain bias, so further prospective multicenter studies are warranted. In comparison, our study has preliminarily explored a new treatment model in patients with transformed SCLC.

Prospective studies with larger sample sizes are expected in the future. Due to the limitation of availability of initially-transformed SCLC/NEC samples, the stability of the PDO model from transformed SCLC cannot be fully established, and the results of drug testing by PDOs also need to be further verified by more clinical evidence. In addition, further exploration is needed in the future by larger sample sizes and other models *in vitro*.

Conclusions

In summary, *EGFR* 19del or L858R-mutant proteins could be constantly expressed, and EGFR pathway still existed in *EGFR*-mutant transformed SCLC/NEC with a common clonal origin from the baseline LUAD. Taking together, these molecular characteristics potentially favored clinical efficacy in transformed SCLC/NEC treated with the combo regimen. However, the mechanism of the combined regimen still needs to be further explored by multicenter clinical studies with larger sample sizes.

Acknowledgments

Part of our study have been accepted as mini oral presentation at the World Conference on Lung Cancer 2020. We thank all the patients who participated in this study and their families. We also thank Tongshu Biotech (Shanghai, China) for their help with WES and data analysis. Besides, we thank Burning Rock Biotech and Nanjing Geneseeq Technology Inc. (Nanjing, China) for their valuable assistance in NGS data analysis and interpretation. Finally, the authors thank Accurate International Biotechnology Co. (Guangzhou, China) for their assistance with organoid culturing and drug testing.
Funding: This study was supported by the High-Level Hospital Construction Project (No. DFJH201809 to Yang JJ), the National Natural Science Foundation of China (No. 81972164 to Yang JJ), the Natural Science Foundation of Guangdong Province (No. 2019A1515010931 to Yang JJ) and Key Lab System Project of Guangdong Science and Technology Department-Guangdong Provincial Key Lab of Translational Medicine in Lung Cancer (No. 2017B030314120 to Wu YL).

Footnote

Reporting Checklist: The authors have completed the MDAR reporting checklist. Available at https://jtd.amegroups.com/article/view/10.21037/jtd-23-161/rc

Data Sharing Statement: Available at https://jtd.amegroups.com/article/view/10.21037/jtd-23-161/dss

Conflicts of Interest: All authors have completed the ICMJE uniform disclosure form (available at https://jtd.amegroups.com/article/view/10.21037/jtd-23-161/coif). YLW reports that he receives funding support for Key Lab System Project of Guangdong Science and Technology Department-Guangdong Provincial Key Lab of Translational Medicine in Lung Cancer (No. 2017B030314120). JJY reports that he receives funding support for the High-Level Hospital Construction Project (No. DFJH201809), the National Natural Science Foundation of China (No. 81972164) and the Natural Science Foundation of Guangdong Province (No. 2019A1515010931). The other authors have no conflicts of interest to declare.

Ethical Statement: The authors are accountable for all aspects of the work in ensuring that questions related to the accuracy or integrity of any part of the work are appropriately investigated and resolved. The study was conducted in accordance with the Declaration of Helsinki (as revised in 2013). Ethical approval was obtained from the Ethical Review Committee of Guangdong Provincial People's Hospital [No. GDREC2019217H(R1)]. Furthermore, written informed consent was obtained from the patients or their immediate family members.

References

1. Maemondo M, Inoue A, Kobayashi K, et al. Gefitinib or chemotherapy for non-small-cell lung cancer with mutated EGFR. N Engl J Med 2010;362:2380-8.
2. Zhou C, Wu YL, Chen G, et al. Erlotinib versus chemotherapy as first-line treatment for patients with advanced EGFR mutation-positive non-small-cell lung

cancer (OPTIMAL, CTONG-0802): a multicentre, open-label, randomised, phase 3 study. Lancet Oncol 2011;12:735-42.
3. Wu YL, Zhou C, Hu CP, et al. Afatinib versus cisplatin plus gemcitabine for first-line treatment of Asian patients with advanced non-small-cell lung cancer harbouring EGFR mutations (LUX-Lung 6): an open-label, randomised phase 3 trial. Lancet Oncol 2014;15:213-22.
4. Wu YL, Cheng Y, Zhou X, et al. Dacomitinib versus gefitinib as first-line treatment for patients with EGFR-mutation-positive non-small-cell lung cancer (ARCHER 1050): a randomised, open-label, phase 3 trial. Lancet Oncol 2017;18:1454-66.
5. Ramalingam SS, Vansteenkiste J, Planchard D, et al. Overall Survival with Osimertinib in Untreated, EGFR-Mutated Advanced NSCLC. N Engl J Med 2020;382:41-50.
6. Oxnard GR, Hu Y, Mileham KF, et al. Assessment of Resistance Mechanisms and Clinical Implications in Patients With EGFR T790M-Positive Lung Cancer and Acquired Resistance to Osimertinib. JAMA Oncol 2018;4:1527-34.
7. Engelman JA, Zejnullahu K, Mitsudomi T, et al. MET amplification leads to gefitinib resistance in lung cancer by activating ERBB3 signaling. Science 2007;316:1039-43.
8. Takezawa K, Pirazzoli V, Arcila ME, et al. HER2 amplification: a potential mechanism of acquired resistance to EGFR inhibition in EGFR-mutant lung cancers that lack the second-site EGFRT790M mutation. Cancer Discov 2012;2:922-33.
9. Sequist LV, Waltman BA, Dias-Santagata D, et al. Genotypic and histological evolution of lung cancers acquiring resistance to EGFR inhibitors. Sci Transl Med 2011;3:75ra26.
10. Schoenfeld AJ, Chan JM, Kubota D, et al. Tumor Analyses Reveal Squamous Transformation and Off-Target Alterations As Early Resistance Mechanisms to First-line Osimertinib in EGFR-Mutant Lung Cancer. Clin Cancer Res 2020;26:2654-63.
11. Iams WT, Beckermann KE, Almodovar K, et al. Small Cell Lung Cancer Transformation as a Mechanism of Resistance to PD-1 Therapy in KRAS-Mutant Lung Adenocarcinoma: A Report of Two Cases. J Thorac Oncol 2019;14:e45-8.
12. Sehgal K, Varkaris A, Viray H, et al. Small cell transformation of non-small cell lung cancer on immune checkpoint inhibitors: uncommon or under-recognized? J Immunother Cancer 2020;8:e000697.
13. Shen Q, Qu J, Sheng L, et al. Case Report: Transformation From Non-Small Cell Lung Cancer to Small Cell Lung Cancer During Anti-PD-1 Therapy: A Report of Two Cases. Front Oncol 2021;11:619371.
14. Cha YJ, Cho BC, Kim HR, et al. A Case of ALK-Rearranged Adenocarcinoma with Small Cell Carcinoma-Like Transformation and Resistance to Crizotinib. J Thorac Oncol 2016;11:e55-8.
15. Fujita S, Masago K, Katakami N, et al. Transformation to SCLC after Treatment with the ALK Inhibitor Alectinib. J Thorac Oncol 2016;11:e67-72.
16. Takegawa N, Hayashi H, Iizuka N, et al. Transformation of ALK rearrangement-positive adenocarcinoma to small-cell lung cancer in association with acquired resistance to alectinib. Ann Oncol 2016;27:953-5.
17. Fares AF, Lok BH, Zhang T, et al. ALK-rearranged lung adenocarcinoma transformation into high-grade large cell neuroendocrine carcinoma: Clinical and molecular description of two cases. Lung Cancer 2020;146:350-4.
18. Oser MG, Niederst MJ, Sequist LV, et al. Transformation from non-small-cell lung cancer to small-cell lung cancer: molecular drivers and cells of origin. Lancet Oncol 2015;16:e165-72.
19. Calbó J, Meuwissen R, van Montfort E, et al. Genotype-phenotype relationships in a mouse model for human small-cell lung cancer. Cold Spring Harb Symp Quant Biol 2005;70:225-32.
20. Travis WD, Brambilla E, Burke AP, et al. Introduction to The 2015 World Health Organization Classification of Tumors of the Lung, Pleura, Thymus, and Heart. J Thorac Oncol 2015;10:1240-2.
21. Baine MK, Febres-Aldana CA, Chang JC, et al. POU2F3 in SCLC: Clinicopathologic and Genomic Analysis With a Focus on Its Diagnostic Utility in Neuroendocrine-Low SCLC. J Thorac Oncol 2022;17:1109-21.
22. Norkowski E, Ghigna MR, Lacroix L, et al. Small-cell carcinoma in the setting of pulmonary adenocarcinoma: new insights in the era of molecular pathology. J Thorac Oncol 2013;8:1265-71.
23. Offin M, Chan JM, Tenet M, et al. Concurrent RB1 and TP53 Alterations Define a Subset of EGFR-Mutant Lung Cancers at risk for Histologic Transformation and Inferior Clinical Outcomes. J Thorac Oncol 2019;14:1784-93.
24. Niederst MJ, Sequist LV, Poirier JT, et al. RB loss in resistant EGFR mutant lung adenocarcinomas that transform to small-cell lung cancer. Nat Commun 2015;6:6377.
25. Li R, Jiang L, Zhou X, et al. Pseudo-small cell transformation in EGFR-mutant adenocarcinoma. Lung

Cancer 2021;153:120-5.
26. Levacq D, D'Haene N, de Wind R, et al. Histological transformation of ALK rearranged adenocarcinoma into small cell lung cancer: A new mechanism of resistance to ALK inhibitors. Lung Cancer 2016;102:38-41.
27. Marcoux N, Gettinger SN, O'Kane G, et al. EGFR-Mutant Adenocarcinomas That Transform to Small-Cell Lung Cancer and Other Neuroendocrine Carcinomas: Clinical Outcomes. J Clin Oncol 2019;37:278-85.
28. Wang W, Xu C, Chen H, et al. Genomic alterations and clinical outcomes in patients with lung adenocarcinoma with transformation to small cell lung cancer after treatment with EGFR tyrosine kinase inhibitors: A multicenter retrospective study. Lung Cancer 2021;155:20-7.
29. Suda K, Murakami I, Sakai K, et al. Small cell lung cancer transformation and T790M mutation: complimentary roles in acquired resistance to kinase inhibitors in lung cancer. Sci Rep 2015;5:14447.
30. Ku SY, Rosario S, Wang Y, et al. Rb1 and Trp53 cooperate to suppress prostate cancer lineage plasticity, metastasis, and antiandrogen resistance. Science 2017;355:78-83.
31. Quintanal-Villalonga Á, Chan JM, Yu HA, et al. Lineage plasticity in cancer: a shared pathway of therapeutic resistance. Nat Rev Clin Oncol 2020;17:360-71.
32. Quintanal-Villalonga A, Taniguchi H, Zhan YA, et al. Multiomic Analysis of Lung Tumors Defines Pathways Activated in Neuroendocrine Transformation. Cancer Discov 2021;11:3028-47.
33. Zhou Q, Zhang XC, Chen ZH, et al. Relative abundance of EGFR mutations predicts benefit from gefitinib treatment for advanced non-small-cell lung cancer. J Clin Oncol 2011;29:3316-21.
34. Mao X, Zhang Z, Zheng X, et al. Capture-Based Targeted Ultradeep Sequencing in Paired Tissue and Plasma Samples Demonstrates Differential Subclonal ctDNA-Releasing Capability in Advanced Lung Cancer. J Thorac Oncol 2017;12:663-72.
35. Yang Z, Yang N, Ou Q, et al. Investigating Novel Resistance Mechanisms to Third-Generation EGFR Tyrosine Kinase Inhibitor Osimertinib in Non-Small Cell Lung Cancer Patients. Clin Cancer Res 2018;24:3097-107.
36. Xie T, Li Y, Ying J, et al. Whole exome sequencing (WES) analysis of transformed small cell lung cancer (SCLC) from lung adenocarcinoma (LUAD). Transl Lung Cancer Res 2020;9:2428-39.
37. Chen JH, Chu XP, Zhang JT, et al. Genomic characteristics and drug screening among organoids derived from non-small cell lung cancer patients. Thorac Cancer 2020;11:2279-90.
38. Ferrer L, Giaj Levra M, Brevet M, et al. A Brief Report of Transformation From NSCLC to SCLC: Molecular and Therapeutic Characteristics. J Thorac Oncol 2019;14:130-4.
39. Tang K, Jiang N, Kuang Y, et al. Overcoming T790M mutant small cell lung cancer with the third-generation EGFR-TKI osimertinib. Thorac Cancer 2019;10:359-64.
40. Yang H, Liu L, Zhou C, et al. The clinicopathologic of pulmonary adenocarcinoma transformation to small cell lung cancer. Medicine (Baltimore) 2019;98:e14893.
41. Shen R, Seshan VE. FACETS: allele-specific copy number and clonal heterogeneity analysis tool for high-throughput DNA sequencing. Nucleic Acids Res 2016;44:e131.
42. Hynes NE, Lane HA. ERBB receptors and cancer: the complexity of targeted inhibitors. Nat Rev Cancer 2005;5:341-54.
43. Kim M, Mun H, Sung CO, et al. Patient-derived lung cancer organoids as in vitro cancer models for therapeutic screening. Nat Commun 2019;10:3991.
44. Shi R, Radulovich N, Ng C, et al. Organoid Cultures as Preclinical Models of Non-Small Cell Lung Cancer. Clin Cancer Res 2020;26:1162-74.
45. Kim SY, Kim SM, Lim S, et al. Modeling Clinical Responses to Targeted Therapies by Patient-Derived Organoids of Advanced Lung Adenocarcinoma. Clin Cancer Res 2021;27:4397-409.

Cite this article as: Zhang SL, Zhang CY, Chen YQ, Li YF, Xie Z, Zhang XC, Zhou Q, Zhong WZ, Huang J, Sun H, Zheng MY, Xiao FM, Yan HH, Lu DX, Lv ZY, Wu YL, Chen HJ, Yang JJ. Expression of *EGFR*-mutant proteins and genomic evolution in *EGFR*-mutant transformed small cell lung cancer. J Thorac Dis 2023;15(9):4620-4635. doi: 10.21037/jtd-23-161